# Hybrid dc–ac electron gun for fs-electron pulse generation

**L Veisz**[1,4]**, G Kurkin**[2]**, K Chernov**[2]**, V Tarnetsky**[2]**, A Apolonski**[3]**,
F Krausz**[1,3] **and E Fill**[1]

[1] Max-Planck-Institut für Quantenoptik, Hans-Kopfermann-Strasse 1,
D-85748 Garching, Germany
[2] Budker Institute for Nuclear Physics, 630090 Novosibirsk, Russia
[3] Department für Physik der Ludwig-Maximilians-Universität München,
Am Coulombwall 1, D-85748 Garching, Germany
E-mail: laszlo.veisz@mpq.mpg.de

**Abstract.** We present a new concept of an electron gun for generating subrelativistic few-femtosecond (fs) electron pulses. The basic idea is to utilize a dc acceleration stage combined with an RF cavity, the ac field of which generates an electron energy chirp for bunching at the target. To reduce space charge (SC) broadening the number of electrons in the bunch is reduced and the gun is operated at a megahertz (MHz) repetition rate for providing a high average number of electrons at the target. Simulations of the electron gun were carried out under the condition of no SC and with SC assuming various numbers of electrons in the bunch. Transversal effects such as defocusing after the dc extraction hole were also taken into account. A detailed analysis of the sensitivity of the pulse duration to various parameters was performed to test the realizability of the concept. Such electron pulses will allow significant advances in the field of ultrafast electron diffraction.

[4] Author to whom any correspondence should be addressed.

IOP Institute of Physics Φ DEUTSCHE PHYSIKALISCHE GESELLSCHAFT

## Contents

## 1. Introduction

Ultrafast electron diffraction (UED) is a powerful diagnostic method which has provided impressive results in molecular dynamics and ultrafast chemistry [1]–[5]. At present, however, the temporal resolution of UED is limited to several 100 fs, mainly due to space charge (SC)-induced broadening of the electron pulse. The generation of few-femtosecond (fs) electron pulses would significantly advance this technique, permitting diffraction imaging of the fastest structural dynamics of molecules and solids.

A number of suggestions have been made to improve the temporal resolution of UED and generate sub-100-fs or even shorter electron pulses. These include using single electron pulses at a megahertz (MHz) repetition rate, or a very short electron gun to eliminate SC-induced broadening [4, 6, 7]. Furthermore, the generation of attosecond electron bunches by means of high-intensity laser pulses [8] has been proposed. Slicing an ultrashort electron pulse out of a longer one by femtosecond electron pulse gating with surface plasmons [9] or by ponderomotive deflection [10] has also been proposed. Another suggestion is sub-fs pulse generation by electron bunching using a 'temporal lens' [11] or a cavity with a curve-shaped wall [12]. More recently, electron pulses emitted from a sharp tungsten tip by means of a few-cycle laser pulse have been observed and simulations indicate that single electron pulses of sub-fs duration may be generated in this way [13]. Electron diffraction using 5.4 MeV electrons has also recently been demonstrated and it has been argued that SC broadening may be overcome by utilizing relativistic electrons [14].

In a recent paper, we presented a novel approach to generating several fs to sub-fs subrelativistic electron pulses for UED [7]. The basic idea is borrowed from accelerator technology and consists of using an ac field generated in a cylindrical RF resonator, a so-called pill-box cavity, for acceleration. It was shown that initiating the electrons with a fs-laser at the appropriate phase of the ac cycle generates an energy chirp in the electron pulse which leads to 'temporal focusing' of the electrons at some distance of propagation. The pill-box cavity allows the parameters of the electric field to be chosen in a wide range for optimizing the electron pulse duration at a specified distance from the target. Simulations with 30 electrons in the bunch yielded a pulse duration of 70 fs, whereas for single electrons, i.e. for the case without SC, 'effective' pulse durations in the attosecond range were predicted. An effective pulse duration may be defined as the standard deviation of the arrival time of the electrons averaged over a large number of events.
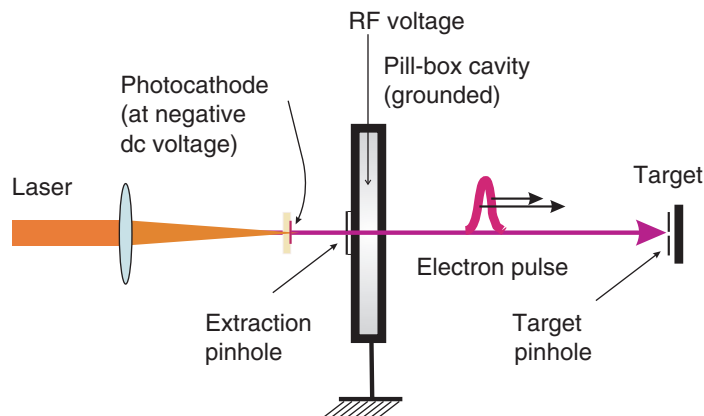
**Figure 1.** Basic arrangement of an electron gun using dc–ac acceleration. The photocathode consists of a quartz plate coated with a thin layer of suitable metal. Electrons enter and leave the pill-box cavity through small holes on either side. The region to the target is field-free.

A shortcoming of this approach is that it requires rather high RF power to generate the acceleration field in the cavity [15]. At room temperature the RF power at 5 GHz is in the range of some tens of kilowatts, which can be reduced by a factor of 5 at the temperature of liquid nitrogen. Nevertheless, continuous wave operation of a cavity at such a power level would constitute a considerable challenge.

In this paper we present a modification of the ac-acceleration approach, which essentially solves the RF power problem. The new method utilizes a combination of dc and ac fields, thus dividing the tasks of acceleration of the electrons and generating the chirp required for bunching between two parts of the system. An appropriate chirp of the electron pulse means that the electrons which are leading the bunch have lower energy, thus propagating with slower velocity whereas the electrons trailing the bunch have a higher energy and thus propagate faster. As the simulations show, the new approach has two more advantages, viz. the pulse duration remains short even with a fair amount of SC and, moreover, the sensitivity to a timing error between the laser and the RF cavity is greatly reduced.

## 2. The dc–ac concept

The basic principle of the new electron gun is shown in figure 1. Initial acceleration is achieved with a dc gap similar to those used in state-of-the-art photo-guns: a photocathode consisting of a quartz plate with a thin layer of metal (e.g. gold, silver or copper) is illuminated from the rear side by a fs-laser. Either the photon energy of the laser has to be above the work function of the metal (which typically requires the 3rd harmonic of a titanium sapphire laser) or one may use multiphoton photoemission. The anode, a distance of about a centimetre away, consists of a pill-box cavity excited in its $TM_{010}$ mode. The ac fields are generated in this cylindrical RF resonator, pill-box cavity, by an RF generator as in a conventional accelerator and are applied continuously and not pulsed. For this mode the electric field is longitudinal and the magnetic field is azimuthal, with Bessel-function radial distributions [16, 17]. The electric field has its maximum on axis. Both fields are constant over the length of the cavity and oscillate with the

resonance frequency as given by

$$\nu_{010}(\text{Hz}) = 1.147 \times 10^{10}/r_0, \tag{1}$$

where $r_0$ is the radius of the cavity in centimetres. An important feature is the fact that the resonance frequency is independent of the cavity length. The electrons enter and exit the cavity through small holes in the center. The space between the cavity and the target is field-free. Upon traversing the RF cavity the electrons acquire a chirp, with the effect that the pulse duration goes through a minimum at a certain distance from the cavity.

Neglecting SC, one can calculate the basic parameters of the dc–ac gun analytically. Let the dc acceleration energy be $U$, the RF frequency be $\nu$, and the distance from the end of the pill-box to the target be $L$. By solving the nonrelativistic equation of motion it can readily be verified that an initial energy $U_i$ of electrons released from the cathode will result in a temporal advancement at the end of the dc field, given by

$$\Delta t \, (\text{s}) = 3.37 \times 10^{-9}(U_i)^{1/2}d/U, \tag{2}$$

as compared to those released with zero initial energy. Here $d$ is the width of the dc gap in millimetres, and $U_i$ and $U$ are in electron volts (eV). Equation (2) is derived on the assumption that $U_i \ll U$.

To make electrons emitted with zero initial energy arrive at the target at the same time, the 'advanced' electrons need to propagate longer by a time $\Delta t$, i.e. their velocity $u$ must be reduced by $\Delta u = u\Delta t/T$, where $T = L/u$ is the time of propagation to the target. The required velocity change is therefore given by

$$\Delta u = u^2 \Delta t/L \tag{3}$$

and, using the nonrelativistic relations $\Delta u = (1/2)\Delta U/U$ and $u = (2eU/m)^{1/2}$, one obtains for the required difference in electron energy

$$\Delta U(\text{eV}) = \sqrt{8e/m}\frac{\Delta t U^{3/2}}{L}. \tag{4}$$

In this equation $e$ is the elementary charge and $m$ is the electron mass. If the electrons reach the cavity at the time when the field goes through zero, one can write the cavity voltage as $U_{\text{cav}} = U_{\text{RF}}\sin(2\pi\nu t)$ and, taking $\Delta t \ll 1/\nu$, approximate the required cavity voltage amplitude with

$$U_{\text{RF}} = \Delta U/(2\pi\nu\,\Delta t). \tag{5}$$

Combining (4) and (5) and evaluating the constants, one obtains

$$U_{\text{RF}} = 1.9 \times 10^5 U^{3/2}/(\nu L), \tag{6}$$

where $U_{\text{RF}}$ is in V, $U$ in electron volts, $\nu$ in Hz and $L$ in metres. Note that in this approximation $U_{\text{RF}}$ is independent of $\Delta t$.

Inserting realistic numbers into the above equations, one may work out the following example. With a typical initial energy spread of the electrons of $U_i = 1\,\text{eV}$ and a dc voltage of $40\,\text{kV}$ over a gap width of $d = 10\,\text{mm}$, the temporal advancement from (2) is $\Delta t = 840\,\text{fs}$, and for a distance to the target of $L = 0.1\,\text{m}$ the energy difference needed to compensate for that time difference becomes $\Delta U = 80\,\text{eV}$. At an RF frequency $\nu = 5\,\text{GHz}$ equation (6) yields a cavity voltage amplitude $U_{\text{RF}} = 3.04\,\text{kV}$. Thus, the required electron velocity spread can be generated with rather modest cavity voltage, which can be achieved with an RF power of

about 100 W. The use of an 'omega'-shaped cavity, with optimized shunt resistance [18], will reduce the RF power to a level of about 10 W, making it possible to use semiconductor drivers with high stability.

A point of concern for generating fs electron pulses is the transverse spread of the electron beam. This effect can be analytically estimated using the relation for the focal length $f$ of an extraction hole, given by [19]

$$f = 4U/[e(E_2 - E_1)], \tag{7}$$

where $E_1$ and $E_2$ are fields before and behind extraction hole, respectively. Realizing that the field in the cavity is much smaller than the dc acceleration field one can neglect $E_2$ in (7) and, using $U = eE_1d$ the focal length is simply given by

$$f = -4d. \tag{8}$$

This is the well-known result that the exit hole constitutes a weak negative lens for the electrons.

With the result of equation (8) one can now estimate the amount of broadening of an electron pulse due to transverse spreading of the electron bunch. Since the field in the cavity is comparatively small and the region to the target is field-free, the effect of the exit hole of the cavity can be neglected and only the lensing effect due to the entrance hole must be considered. At a target distance $L$ a narrow beam of radius $r_0$ would spread to a radius of $r_t = r_0(1 + L/4d)$, resulting in a path difference of approximately $\Delta L = Lr_0^2/(32d^2)$ between the central part and the rim of the beam. For the time difference $\Delta L/u$ one therefore derives the expression

$$\Delta \tau_t = Lr_0^2/(32ud^2). \tag{9}$$

Taking the parameters from above, i.e. $d = 1\,\text{cm}$, $u = 1.12 \times 10^{10}\,\text{cm s}^{-1}$ for 40 keV electrons, $L = 10\,\text{cm}$ and assuming an initial radius of the beam of $r_0 = 25\,\mu\text{m}$, one derives a pulse broadening of 0.17 fs while for 150 $\mu$m radius the result is 6.1 fs. This implies that transverse effects could lead to pulse broadening comparable to the shortest pulse duration depending on the beam radius at the exit of the dc field when working in the femtosecond range. When aiming at attosecond pulses this effect must be considered in any case (see section 4).

## 3. Simulations of dc–ac acceleration

The dc–ac photo-gun was simulated by means of the General Particle Tracer (GPT) code (online at http://www.pulser.nl/gpt), a well-established simulation tool for designing accelerator beam lines. It provides full 3D particle tracking and allows beam line components to be arbitrarily positioned and oriented. SC effects are treated with the model described in [20] but can be switched off to simulate purely ballistic propagation. In this part of the simulations we neglect the defocusing originating from the exit holes, in order to analyze the effect of bunching with and without SC. The defocusing effect will be considered in detail in section 4.

The following parameters were used for the simulation: electrons are emitted from a circular spot at the cathode with a Gaussian distribution with a full width at half maximum (FWHM) of 20 $\mu$m. The emission occurs at times $-13\,\text{fs} < t < 13\,\text{fs}$ with a truncated Gaussian temporal distribution with a FWHM of 10 fs centered at $t = 0$. The laser pulse duration is not a sensitive parameter in these simulations, since it is much shorter than the temporal advancement resulting from the initial velocity spread of the electrons. The dc acceleration stage was 10 mm long with an applied voltage of 40 kV. Note that this voltage is well below
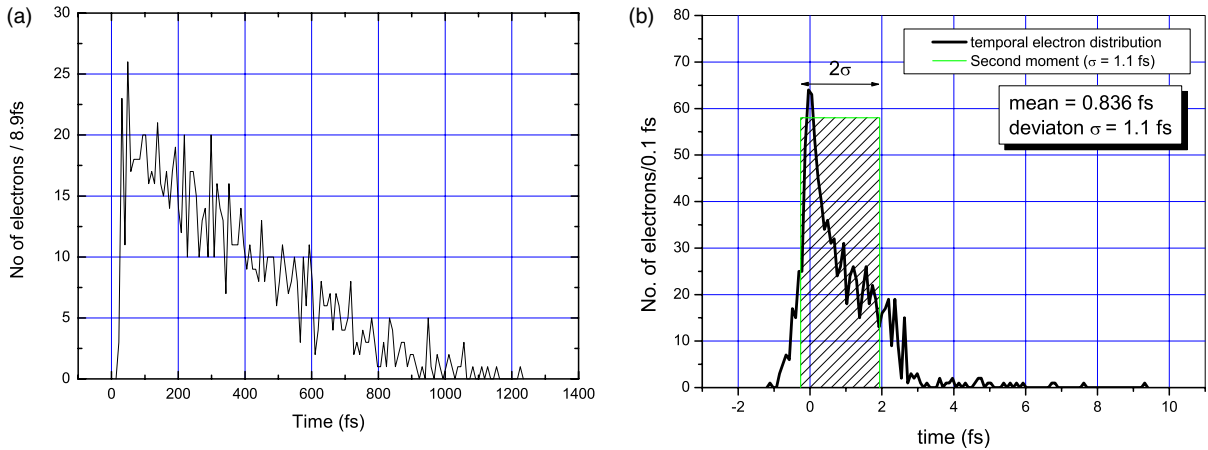
**Figure 2.** (a) Temporal structure of the electron pulse after the dc stage. (b) Temporal electron distribution at position of minimum pulse duration and second-moment pulse duration. The second moment is represented by a hatched bar, centered at the mean, with a width of $2\sigma$.

the limit of $6\,\text{kV}\,\text{mm}^{-1}$ set by field emission and vacuum breakdown [21]. The ac stage was a pill-box cavity 5 mm in length, oscillating at a frequency of 5 GHz with an amplitude of 3.04 kV. The initial energy distribution of electrons emitted from the photocathode was taken to be exponential with a 'temperature' of 1 eV. The electron emission from the cathode was assumed to be isotropic into the half-space.

Runs were carried out with 30, 100, 300 and 1000 electrons in the pulse with SC taken into account and with 1000 electrons and SC switched off. For the runs with no SC 1000 electrons were used to provide a good statistical sample. The phase between the laser pulse envelope on the cathode and the RF oscillation was chosen such that the electrons pass the center of the cavity just at the time of zero voltage (see the condition for deriving (5)). The time it takes the electrons to reach the cavity and for traversing it are 171.5 and 45 ps, respectively. Thus, the time $\tau_C$ for the electrons to reach the center of the cavity is 194 ps and the phase, calculated from the condition of zero voltage at time $\tau_C$, i.e. from the relation $\sin(2\pi\nu\tau_C + \varphi) = 0$, is equal to $-6.1\,\text{rad}$.

In displaying the data the question arises how 'pulse duration' of the electron bunch may be defined. It turns out that the FWHM of a Gaussian fit to the temporal electron bunch distribution would not be a good measure of the pulse duration. This is illustrated in figures 2(a) and (b), which show electron pulse shapes after dc-acceleration and at the target as obtained from the simulations. Figure 2(b) also shows a bar with a width $2\sigma$, where $\sigma$ is the standard deviation of the electron distribution, defined as the second moment. Since this quantity is directly obtained from the simulations, the 'second-moment pulse duration' was chosen to represent the duration of electron pulses in the diagrams that follow. Note that for a Gaussian pulse the relation FWHM/$\sigma = 2.35$ applies.

Second-moment pulse durations as a function of distance as obtained from the simulations are shown in figures 3(a) and (b) for cases with and without SC. After the dc acceleration stage the pulse durations acquire $\sigma$ values of around 250 fs, in fair agreement with the analytical estimate given by equation (2) (compare figure 2(a)). During propagation in the cavity the pulse
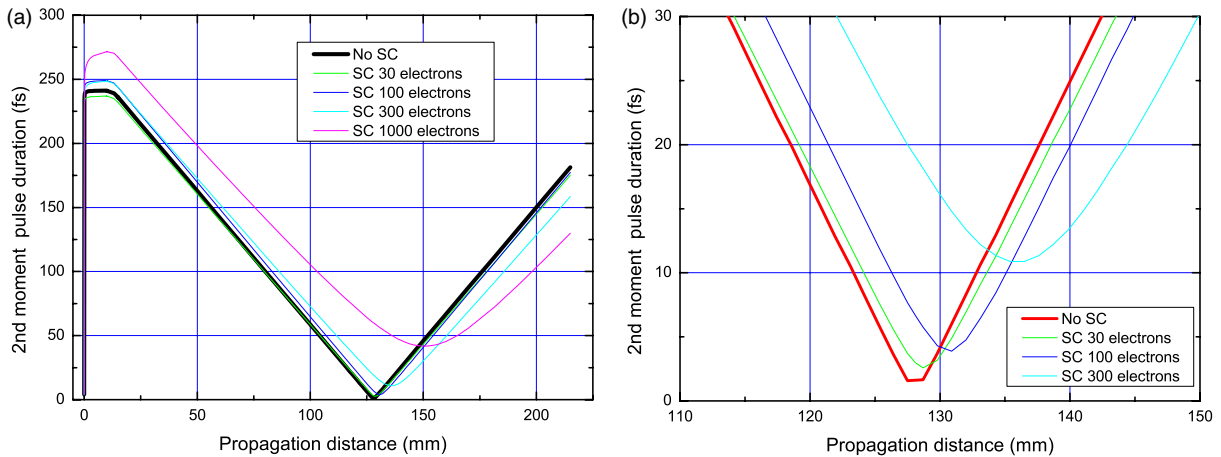
**Figure 3.** (a) Second-moment pulse duration as a function of the distance from the cathode. Results with and without SC are displayed. The numbers after SC give the number of electrons in the bunch. Parameters: dc: 10 mm, 40 kV; ac: 5 mm, 5 GHz, 614 kV m$^{-1}$ and $\varphi = -6.1$ rad. (b) Same as figure 3(a) but region from 110 to 150 mm expanded.

duration changes only very little, but behind the cavity it decreases approximately linearly with distance and reaches a minimum near 130 mm from the cathode (except for the case with SC and 1000 electrons, see below). Runs with increased spatial resolution around the distance of minimum pulse duration yield a pulse duration without SC of $1.05 \pm 0.05$ fs. With increasing number of electrons, the minimum pulse duration becomes longer and occurs at a larger distance from the cathode. However, it is satisfying to see that even with a significant number of electrons in the pulse, bunching still works and the minimum electron pulse duration becomes much smaller than that after the dc acceleration stage. With 30, 100 and 300 electrons in the bunch pulse durations of 2.6, 4 and 11 fs are calculated and with 1000 electrons the minimum pulse duration is 42 fs. In this case, the minimum is relatively flat and the optimum distance is about 150 mm from the cathode.

It follows from the principle of bunching that the ultrashort electron bunch duration comes at the expense of a spread in the energy distribution. Figure 4 displays the electron spectrum at target for the cases of no SC and with SC for 100 electrons in the bunch. The initial energy distribution of the electrons emitted from the cathode is also shown. As apparent from the figure, a total energy spread of 80 eV is generated by the cavity, in agreement with that predicted by (4). Fortunately, such an energy spread, only 0.2% of the mean energy, would not result in significant deterioration of an electron diffraction pattern.

## 4. The effect of the extraction hole

Simulations were made to study the defocusing effect of the extraction hole at the end of the dc field/entrance of the RF cavity. The defocusing originating from the RF cavity field is neglected. An exit hole radius of 500 $\mu$m was assumed with other parameters unchanged compared to figure 3 without SC. The electron distributions in the real space and longitudinal phase space are plotted in figure 5, where $z$ is the propagation direction, $r$ is the transverse direction and
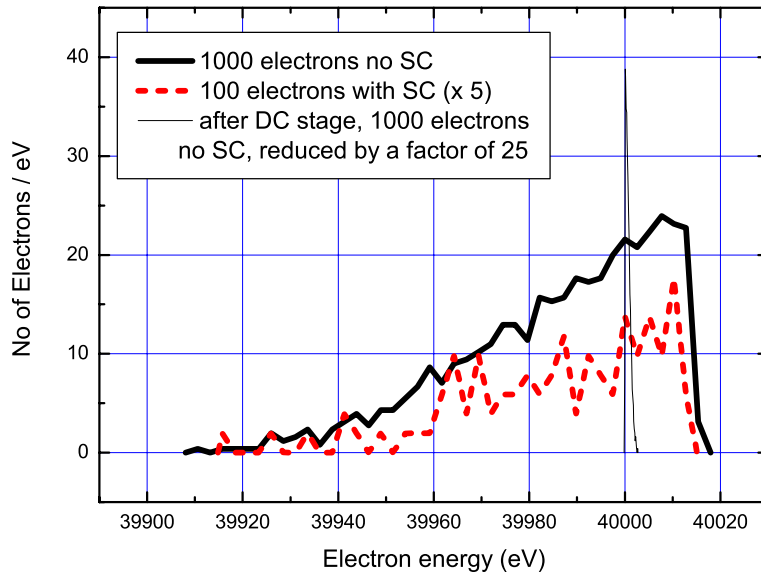
**Figure 4.** Energy distribution of electrons arriving at target for the case of 1000 electrons with no SC and for 100 electrons with SC (multiplied by a factor of 5). The initial energy distribution with a width of 1 eV is also shown. For acceleration parameters see text.

$\beta_z$ is the normalized longitudinal velocity. The electron energy is color coded in the real space pictures and the radial position of the particles is color coded in the phase space plots—red indicates higher and blue lower values. The distributions at the end of the dc field—around 10 mm from the cathode—are shown in figure 5(a). As expected, electrons with higher energies are at the leading edge of the bunch since all particles gain the same energy from the static field. After the RF cavity—15 mm away from the cathode—the situation is reversed and the higher energy electrons get to the trailing edge of the electron pulse as illustrated in figure 5(b), due to the temporally increasing acceleration field. The acquired chirp determines the position where the faster electrons at the back catch up with the slower electrons at the front, which is 128 mm behind the cathode. The distributions approx 2 mm in front of the position of shortest pulse duration, approx. at the position of the shortest bunch duration, and approx. 2 mm behind this position—125.3, 127.5 and 129.8 mm—are depicted in figures 5(c)–(e), correspondingly. It is obvious from the figures that electrons farther from the axis fall behind so elongate the bunch and define the attainable pulse duration. This geometric effect originates from the longer off-axis propagation distances from the cathode to the position of the shortest pulse duration and is basically the same if the electrons are weakly refocused onto the target. The normalized transverse emittance with 500 $\mu$m radius dc hole is $7.8 \times 10^{-3}$ mm mrad.

There are two ways to eliminate this geometrical elongation effect and shorten the pulse. The first way is the application of a curved photo cathode [22], which in the present situation requires extremely precise positioning, shot-to-shot laser pointing stability and cathode production due to the small laser focus. The second way is to use an extra pinhole, for example in front of the target to cut the delayed outer part of the bunch. A consequence of this solution is a reduced electron number reaching the target. This is the solution which we investigate in the following.
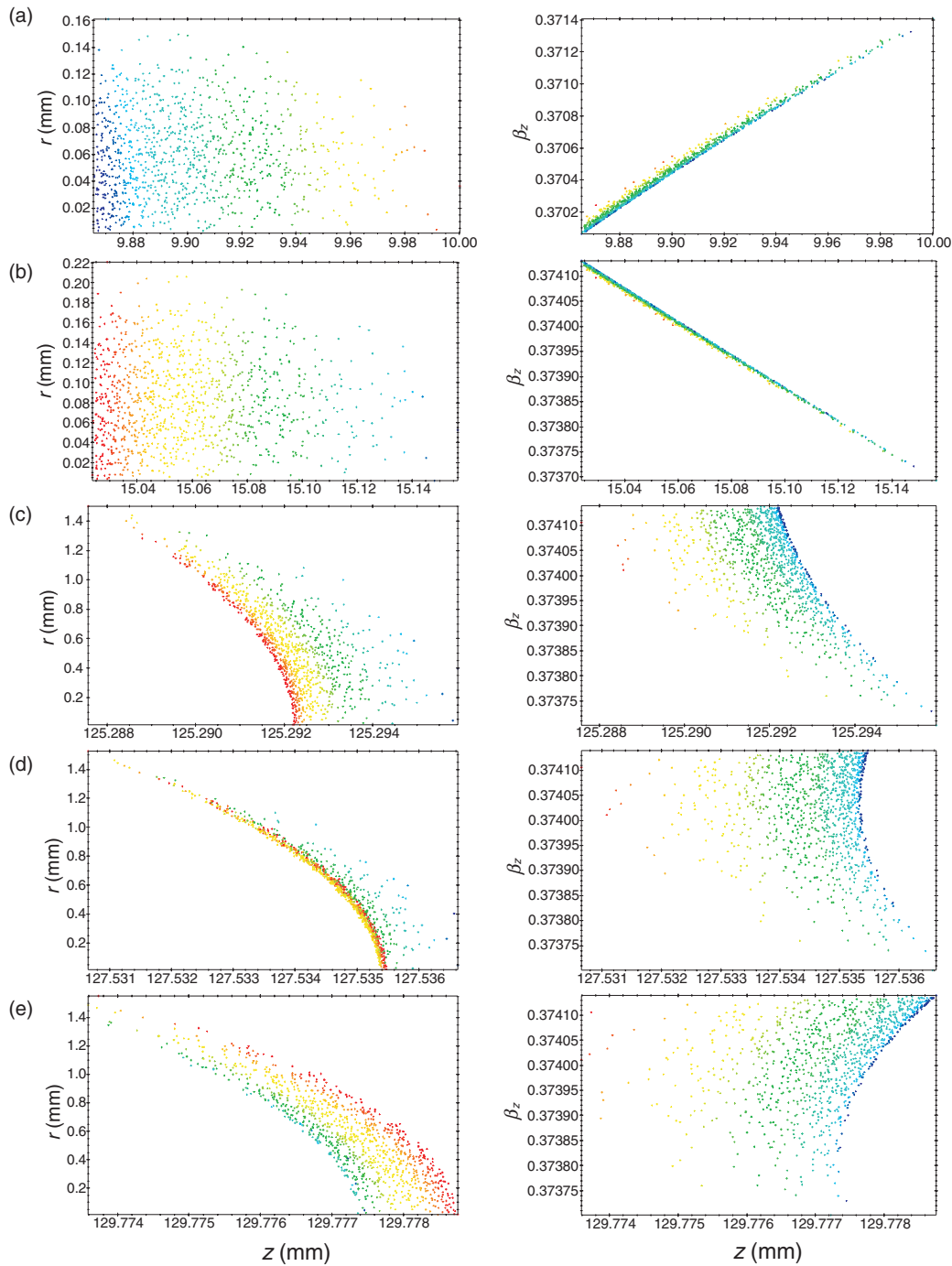
**Figure 5.** Real space and longitudinal phase space snapshots without SC effects, but with defocusing exit hole. Parameters: dc: 10 mm, 40 kV; ac: 5 mm, 5 GHz, 614 kV m$^{-1}$, $\varphi = -6.1$ rad, dc exit hole radius: 500 $\mu$m. The color scale on the real space figures is proportional to the energy of the electron, on the phase space figures is proportional to the radial position of the particle. The $z$ positions correspond to (a) the exit of the dc field, (b) the exit of the ac field, (c) 2.3 mm in front of the position of the shortest bunch duration, (d) the position of the shortest bunch duration and (e) 2.3 mm after the position of the shortest bunch duration.
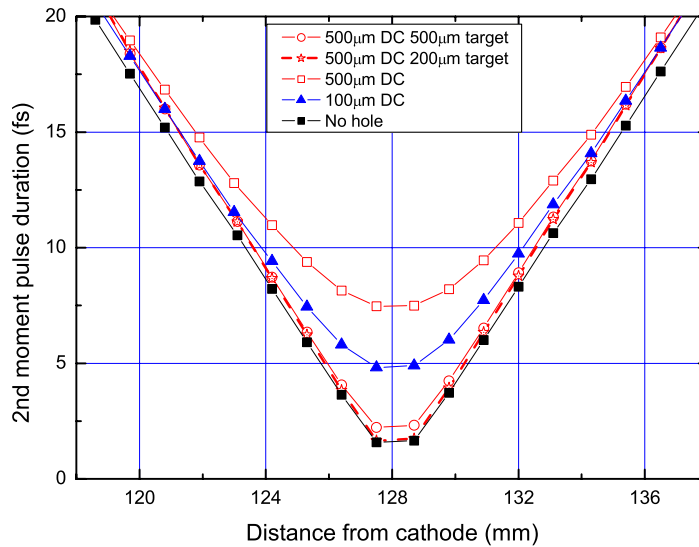
**Figure 6.** Same as figure 3(a) without SC but the defocusing effects of an exit hole after the dc acceleration are also simulated. Region is from 118 to 138 mm expanded. Exit hole radii of 100 and 500 $\mu$m are assumed. A second pinhole with radii 200 and 500 $\mu$m is placed in the case of the 500 $\mu$m exit hole in front of the target.

Figure 6 shows the effect of an extraction hole without SC on the pulse duration versus propagation distance curve after the dc acceleration and the effect of a second pinhole in front of the target to shorten the bunch. The black curve with solid squares is the previous result from figure 3 without hole and a minimum pulse length of $1.05 \pm 0.05$ fs for comparison. The blue line with solid triangles and the red line with open squares are results with a 100 and a 500 $\mu$m radius defocusing hole. Both curves exhibit longer minimum bunch duration—4.7 fs for the 100 $\mu$m and 7.3 fs for the 500 $\mu$m hole—than the simulation without extraction hole demonstrating that the geometrical elongation is significant. The larger the hole diameter the longer is the minimum pulse duration as equation (9) predicts. It should be noted that the beam radius at the extraction hole is about 136 $\mu$m. The red curve with open circles and the thick red dashed curve with open stars illustrate with 500 $\mu$m dc hole the effect of an extra pinhole at 120 mm position with 500 and 200 $\mu$m radius, correspondingly. The 500 $\mu$m radius pinhole transmits 46% of the incident electrons, supports minimum bunch duration of 1.9 fs, and the transmitted beam has a normalized transverse emittance of $4.1 \times 10^{-3}$ mm mrad. While the 200 $\mu$m pinhole transmits 12%, supports minimum bunch duration of $1.09 \pm 0.06$ fs, which is practically the duration without pinhole, i.e. the geometric effects are completely suppressed in this case, and provides a normalized transverse emittance of $1.6 \times 10^{-3}$ mm mrad.

The obtained pulse duration versus propagation distance results including an extraction hole and SC effects using 100 electrons in the bunch are depicted in figure 7. The black curve with solid squares is again the previous result from figure 3 without SC and extraction hole, while the red dashed line with open diamonds represents the results with SC, but without hole and 3.5 fs minimum pulse length from figure 3. The blue line with solid triangles and the thick blue line with open circles shows the curve for 500 $\mu$m radius extraction hole without and with a 500 $\mu$m radius extra pinhole at 120 mm position, respectively. All curves with SC have the
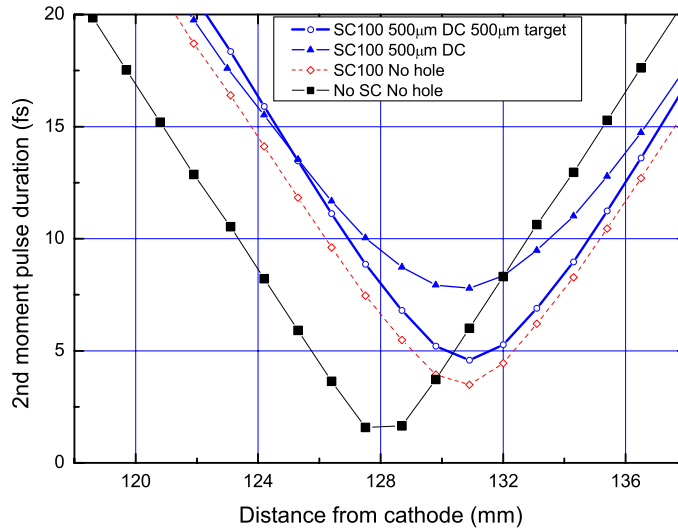
**Figure 7.** Same as figure 3(a) with SC and 100 electrons but the defocusing effects of an exit hole after the dc acceleration are also simulated. Region is from 118 to 138 mm expanded. 500 $\mu$m exit hole radius is assumed. A second pinhole with 500 $\mu$m radius is placed in front of the target.

minimum pulse duration at 130.6 mm, which is due to the extra negative chirp caused by the SC and proves that the chirp is not affected by transversal focusing. The shortest pulse duration without the extra pinhole is 7.8 fs and with the pinhole 4.6 fs with 50% transmission.

The summary of the simulations of the minimal 2nd moment bunch duration as a function of the dc extraction hole radius without SC effects and using 100 electrons and SC effects is plotted in figure 8. The solid black squares represent simulations with various dc extraction hole radii without SC effects. The electron beam radius is 136 $\mu$m at the hole. The simulation without extraction hole is plotted at 21 $\mu$m radius for comparison. The black line is a theoretical estimate for the geometrical elongation using equation (9) with $L = 128$ mm, $u = 1.12 \times 10^{11}$ mm s$^{-1}$ and $d = 10$ mm. As the bunch radius is 136 $\mu$m above this value the size of the extraction hole does not affect the pulse duration. Correspondingly a constant minimal pulse length is expected. The good coincidence between the theoretical estimate and simulations supports the suggestion that the geometrical defocusing is responsible for the longer bunch length. The shortest bunch duration with an extra pinhole with 200 and 500 $\mu$m radii for the 300 and 500 $\mu$m dc extraction hole radius cases are also depicted. The simulations with 100 electrons and SC effects are shown with open red circles for comparison. We conclude that geometrical defocusing might be a quite important effect in obtaining sub-10-fs bunches, but with corresponding measures its temporal elongation effects can be eliminated.

## 5. Stability with respect to parameter variations

The minimum achievable pulse duration is expected to respond sensitively to any changes in the parameters of the accelerating arrangement. In the following section, we scrutinize how small changes in the experimental parameters affect the electron pulse duration. Estimates from the simple theory outlined in section 2 are contrasted with simulation results.
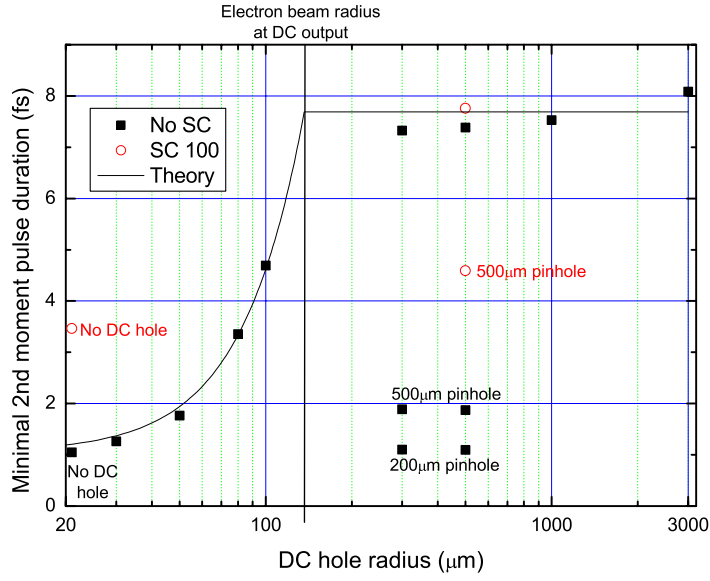
**Figure 8.** Summary of the results with a defocusing exit hole after the dc acceleration. The minimal 2nd moment pulse duration versus dc exit hole radius without SC and with 100 electrons and SC effects. The results without a dc hole are plotted at 21 $\mu$m radius for comparison. Pulse durations at target using a second pinhole with radii 200 and 500 $\mu$m placed in front of the target are also plotted. The black line represents the theoretical estimation from equation (9).

The first parameter to be investigated is the timing of the laser pulse envelope with respect to the phase of the ac-field. The best way to minimize phase jitter is to derive the laser pulses directly from an oscillator locked to the RF driver of the cavity. Recently, lasers with extended oscillator length have been developed and demonstrated to emit sub-100-fs pulses approaching the micro Joule level at a repetition rate of a few MHz [23, 24].

A semi-quantitative calculation of the change in pulse duration with phase error can be carried out by means of the analytical model of section 2. If the phase error is small, the pulse is still temporally focused, but the minimum pulse duration occurs at a different distance from the cavity. In an experiment, however, the pulse duration at a *fixed* distance is relevant, given approximately by

$$\tau = \Delta t \, |\Delta L/L|, \tag{10}$$

where $\Delta t$ is the duration of the electron pulse leaving the cavity and $\Delta L$ is the distance change due to the phase error. Note that in the analytical theory the pulse duration at optimum phase is zero.

From equation (4) the new distance of minimum pulse duration with phase error $\Delta \varphi$ is given by

$$L + \Delta L = \sqrt{8e/m} \frac{\Delta t \, (U + U_{RF} \sin \Delta \varphi)^{3/2}}{\Delta U \cos \Delta \varphi}. \tag{11}$$

Where use has been made of the fact that electrons entering the cavity at phase $\Delta \varphi$ gain an energy of $U_{RF} \sin \Delta \varphi$ and that their energy spread induced by the cavity will be given by
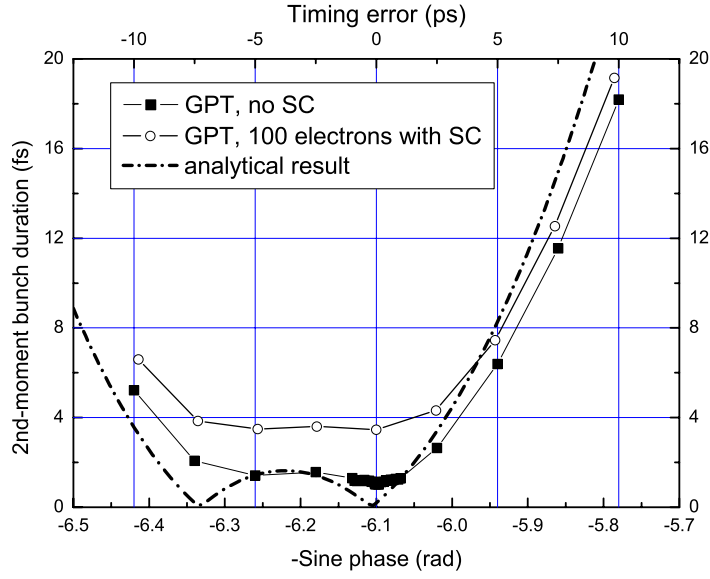
**Figure 9.** Electron pulse duration versus phase and timing error for the case of no SC (solid symbols) and with SC and 100 electrons in the bunch (open symbols) as obtained by GPT simulation. The data for no space charge correspond to a distance of 127.5 mm from the cathode. With SC the distance is 130.7 mm. The result obtained from the analytical model—equation (12)—is also displayed.

$\Delta U \cos \Delta \varphi$. Taking into account that $U \gg U_{\mathrm{RF}}$ and inserting equation (11) into (10) gives for the pulse duration

$$\tau = \Delta t \left| \left( \frac{1 + 3 U_{\mathrm{RF}} \sin \Delta \varphi / 2U}{\cos \Delta \varphi} \right) - 1 \right|. \tag{12}$$

This result can be converted into a dependence on the timing error $\delta t$ by means of the relation $\Delta \varphi = 2 \pi \nu \, \delta t$.

Equation (12) shows that the pulse duration will change asymmetrically with the phase error $\Delta \varphi$. For a negative phase error $\Delta \varphi$ the denominator decreases, but $\cos \Delta \varphi$ also decreases. These changes partially cancel each other and the pulse duration will exhibit only a slight variation. For positive $\Delta \varphi$ the denominator increases whereas $\cos \Delta \varphi$ decreases, resulting in a monotonic increase in the pulse duration.

In figure 9, the pulse duration versus timing error from equation (12) as well as the results from GPT simulations are displayed. For the analytical result an input electron pulse duration $\Delta t = 250$ fs, as taken from the simulations at optimum phase (see figure 3(a)), was assumed. The asymmetry of the pulse duration as a function of the timing error as derived above is also seen in the GPT simulation results. For the case of no SC the agreement with the analytical theory is very good. Note that no adjustable parameter has been used. With and without SC a timing error of several picoseconds is tolerated. To keep the pulse duration below 10 fs a timing error of $-12$ and $+7$ ps is allowed.

A second issue of concern is the sensitivity to variations in the amplitude of the RF cavity field. Again, the effect can be estimated analytically. Assuming that the electrons enter the cavity without phase error (i.e. at $\varphi = 0$ and realizing that the energy spread generated by the cavity is now given by $\Delta U(1 + \delta U_{\mathrm{RF}} / U_{\mathrm{RF}})$, where $\delta U_{\mathrm{RF}} / U_{\mathrm{RF}}$ is the relative error in the RF
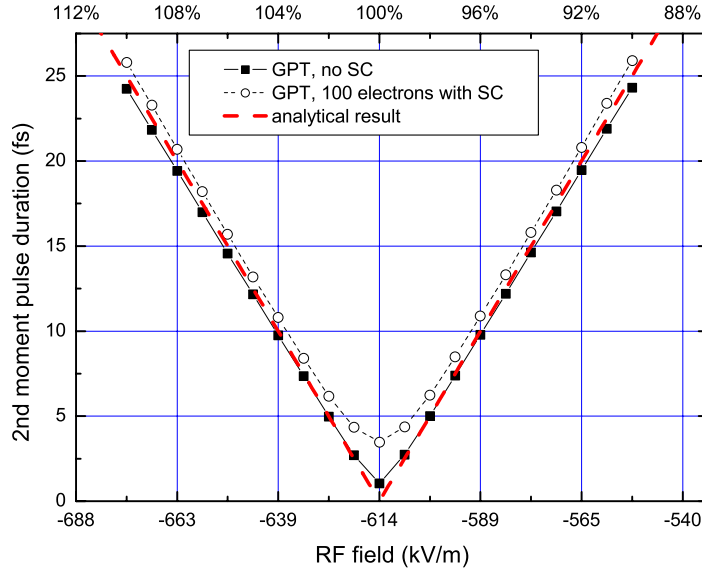
**Figure 10.** Electron pulse duration versus field amplitude in the cavity at constant distance from the cathode. Result for no SC and for 100 electrons in the bunch with SC. The distances are as in figure 5. The analytical estimate from equation (10) is displayed together with the GPT simulation results.

voltage amplitude, one obtains, again using equation (4) for the distance $L$ and equation (10) for the pulse duration,

$$\tau = \Delta t \; |\delta U_{RF}/U_{RF}|. \tag{13}$$

The resulting pulse duration and that from the GPT simulations are plotted in figure 10. As previously, an input pulse duration $\Delta t = 250$ fs was assumed for the analytical calculation. Again, the agreement between simulation and analytical theory is good. The results show that the cavity field amplitude must be stable to about $\pm 4\%$ to avoid an increase in the pulse duration beyond 10 fs.

Finally, we investigate the change in the pulse duration with a change $\delta U$ in the dc acceleration field. For small relative change it is straightforward to derive from the analytical model that the pulse duration is now given by

$$\tau = \Delta t \frac{3 \, |\delta U|}{2U}. \tag{14}$$

Figure 11 displays this equation—with $\Delta t = 250$ fs—together with the GPT simulation result. A stability of $|\delta U/U|$ by better than 4% is required to keep the pulse duration below 10 fs.

These results show that a modest amount of phase jitter as well as realistic values for variations in the dc and ac field strengths still yield few-fs electron pulses. However, one must keep in mind that the temporal jitter of the laser pulses still constitutes a major problem for a pump–probe experiment with fs time resolution: in such an experiment the electron pulse would have to follow exactly the time jitter of the laser pulse. However, the cavity generates a change in the energy of the electrons that makes them invariably arrive at a time corresponding to phase zero, and thus the electron pulse is locked to the cavity oscillation and does not follow variations in timing of the laser pulse. This is illustrated in figure 12 in which the relative arrival time of
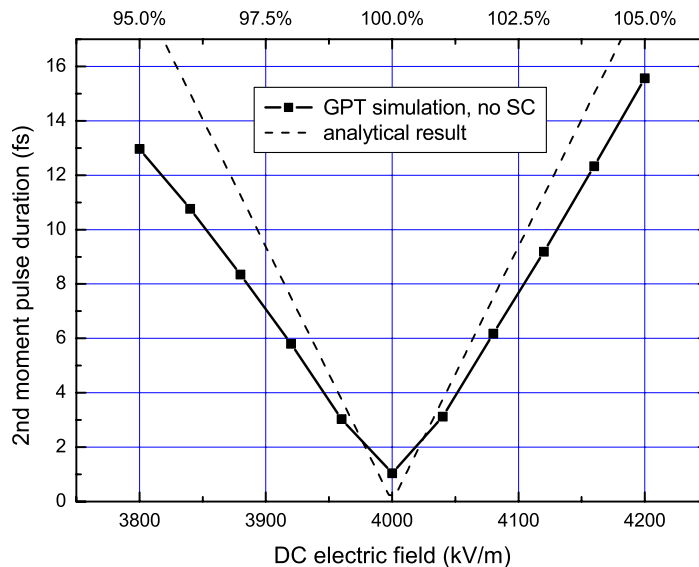
**Figure 11.** Electron pulse duration versus dc field at constant distance from the cathode. The bunch duration relates to the distance at which it is minimum for $4000\,\mathrm{kV\,m^{-1}}$, i.e. 127.5 mm. SC is not taken into account.

the electrons is plotted as a function of the time of emission. As the figure shows the arrival time is almost independent of the time of emission, indicative of locking of the electron pulse to the cavity oscillation. Due to this fact, the temporal resolution of a pump–probe experiment will therefore no longer be determined by the electron pulse duration but by the jitter of the laser. This means that application of the fs-electron pulses in a pump–probe experiment will require special stabilization of the laser repetition rate with respect to the cavity oscillation. We note that locking of a passively mode-locked laser to an RF source has been demonstrated with an rms timing jitter of less than 10 fs [25]. In the present case synchronization can be achieved by driving the RF generator with a high harmonic of the laser repetition rate. An alternative way of synchronization is to tune the RF frequency by means of a signal derived from a phase-sensitive voltage generator.

## 6. Conclusion

In summary, we present a new electron gun design which generates few-fs electron pulses at subrelativistic energies that are suitable for UED. The concept is based on accelerating the electrons by means of a dc field and then inducing an appropriate energy 'chirp' by means of an RF cavity that leads to temporal focusing after a certain distance of propagation. Since the electrons are subrelativistic, a relatively small energy spread induces enough velocity spread to achieve this effect at short distances. The price of temporal focusing is an increase of the spectral bandwidth depending on the position of the focus. In the examples simulated in the present paper this broadening typically amounts to 0.5% of the electron energy. The electron gun generates sub-10-fs pulses with 1–100 electrons in the bunch. To compensate for this relatively low number the pulse repetition rate is projected to be a few MHz. An electron bunch duration of 1 (4) fs is obtained from the simulations using 1 (100) electrons per pulse.
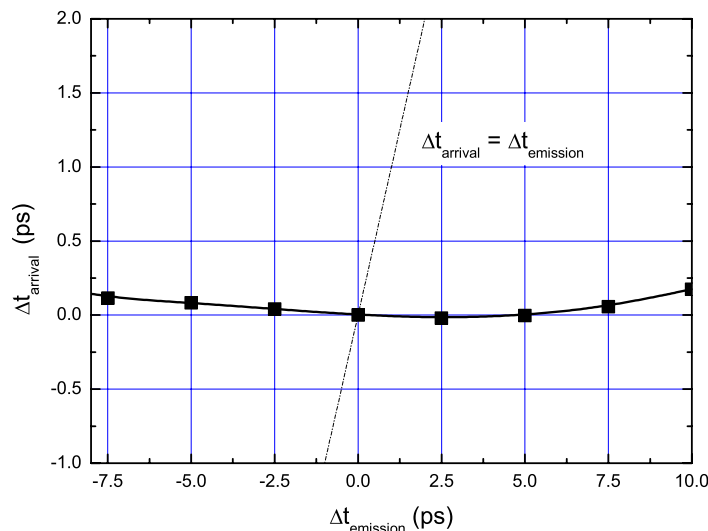
**Figure 12.** Relative arrival time of electrons versus relative time of emission. No SC. The dashed line termed $\Delta t_{\text{arrival}} = \Delta t_{\text{emission}}$, shows the situation if the timing of the electron pulse would follow rigidly that of the laser pulse.

The defocusing originating from the extraction hole at the end of the dc acceleration leads to significant geometrical elongation at the target, which can be completely eliminated with an extra pinhole in front of the target. For the generation of sub-10-fs pulses a temporal jitter between the laser and the RF cycle from $-12$ and $+7$ ps and an RF or dc field amplitude error of 4% can be tolerated. Such a stability is readily achievable in experiments. The possibility of generating electron pulses with few-fs duration will lead to unprecedented temporal resolution in UED experiments.

### Acknowledgment

### References

[1] Helliwell J R and Rentzepis P M 1997 *Time-resolved Diffraction* (Oxford: Clarendon)
[2] Siwick B J, Dwyer J R, Jordan R E and Miller R J D 2003 *Science* **302** 1382
[3] Srinivasan R, Lobastov V A, Ruan C-Y and Zewail A H 2003 *Helv. Chim. Acta* **86** 1763
[4] Dwyer J R, Hebeisen C T, Ernstorfer R, Harb M, Deyirmenjian V B, Jordan R E and Miller R J D 2006 *Phil. Trans. R. Soc.* A **364** 741
[5] Williamson J C, Cao J, Ihee H, Frey H and Zewail A H 1997 *Nature* **386** 159
[6] Lobastov V A, Srinivasan R and Zewail A H 2005 *Proc. Natl Acad. Sci. USA* **102** 7069
[7] Fill E, Veisz L, Apolonski A and Krausz F 2006 *New J. Phys.* **8** 272
[8] Naumova N, Sokolov I, Nees J, Maksimchuk A, Yanovsky V and Mourou G 2004 *Phys. Rev. Lett.* **93** 195003
[9] Irvine S E and Elezzabi A Y 2006 *Opt. Express* **14** 4115

[10]  Baum P and Zewail A H 2006 *Proc. Natl Acad. Sci. USA* **103** 16105

[11]  Monastyrskiy M, Andreev S, Greenfield D, Bryukhnevich G, Tarasov V and Schelev M 2005 Computer modeling of a subfemtosecond photoelectron gun with time-dependent electric field for TRED experiments *High-Speed Photography and Photonics (Proc. SPIE* vol 5580*)* ed L Palsley, S Kleinfelder, D R Snyder and B J Thompson pp 324–34

[12]  Qian B-L and Elsayed-Ali H E 2002 *Phys. Rev.* E **65** 046502

[13]  Hommelhoff P, Kealhofer C and Kasevich M A 2006 *Phys. Rev. Lett.* **97** 247402

[14]  Hastings J B, Rudakov F M, Dowell D H, Schmerge J F, Cardoza J D, Castro J M, Gierman S M, Loos H and Weber P M 2006 *Appl. Phys. Lett.* **89** 184109

[15]  Fill E, Veisz L, Apolonski A and Krausz F 2006 Femtosecond electron gun for diffraction experiment *Millimeter-Wave and Terahertz Photonics (Proc. SPIE, Strasbourg* vol 6194*)* ed D Jäger and A Stöhr

[16]  Wille K 2000 *The Physics of Particle Accelerators* (Oxford: Oxford University Press)

[17]  Wilson E 2001 *An Introduction to Particle Accelerators* (Oxford: Oxford University Press)

[18]  Knapp E A, Knapp B C and Potter J M 1968 *Rev. Sci. Instrum.* **39** 979

[19]  Humphries S Jr 1986 *Principles of Charged Particle Acceleration* (New York: Wiley)

[20]  Pöplau G, van Rienen U, van der Geer S B and de Loos M J 2004 *IEEE Trans. Magn.* **40** 714

[21]  Kinoshita K, Ito M and Suzuki Y 1987 *Rev. Sci. Instrum.* **58** 932

[22]  de Loos M J, van der Geer S B, Saveliev Y M, Pavlov V M, Reitsma A J W, Wiggins S M, Rodier J, Garvey T and Jaroszynski D A 2006 *Phys. Rev. ST Accel. Beams* **9** 084201

[23]  Naumov S, Fernandez A, Graf R, Dombi P, Krausz F and Apolonski A 2005 *New J. Phys.* **7** 216

[24]  Dewald S, Lang T, Schröter C D, Moshammer R, Ullrich J, Siegel M and Morgner U 2006 *Opt. Lett.* **31** 2072

[25]  Ma L-S, Shelton R K, Kapteyn H C, Murnane M M and Ye J 2001 *Phys. Rev.* A **64** 021802